bioRxiv preprint doi: https://doi.org/10.1101/834788; this version posted November 8, 2019. The copyright holder for this preprint (which was not certified by peer review) is the author/funder. All rights reserved. No reuse allowed without permission.

Neurofibromin regulates metabolic rate via neuronal mechanisms in *Drosophila*

Valentina Botero[1], Bethany A. Stahl[2], Eliza C. Grenci[1], Tamara Boto[1], Scarlet J. Park[1], Lanikea B. King[1], Keith R. Murphy[1], Kenneth J. Colodner[3], James A. Walker[4], Alex C. Keene[2], William W. Ja[1], Seth M. Tomchik[1*]

[1]Department of Neuroscience, The Scripps Research Institute, Scripps Florida, Jupiter, FL, USA

[2]Department of Biological Sciences, Florida Atlantic University, Jupiter, FL, USA

[3]Program in Neuroscience and Behavior, Mount Holyoke College, South Hadley, MA, USA

[4]Center for Genomic Medicine, Massachusetts General Hospital, Boston, MA 02114, USA; Cancer Program, Broad Institute of MIT and Harvard, Cambridge, MA 02142, USA

*Correspondence: stomchik@scripps.edu

Keywords: metabolism, pyruvate carboxylase, NF1, Ras, carbon dioxide, oxygen

bioRxiv preprint doi: https://doi.org/10.1101/834788; this version posted November 8, 2019. The copyright holder for this preprint (which was not certified by peer review) is the author/funder. All rights reserved. No reuse allowed without permission.

ABSTRACT

Neurofibromatosis type 1 (NF1) is a genetic disorder predisposing patients to a range of features, the most characteristic of which include areas of abnormal skin pigmentation and benign tumors associated with peripheral nerves, termed neurofibromas. Less common, but more serious symptoms also include malignant peripheral nerve sheath tumors, other malignancies, and learning disabilities. The *NF1* gene encodes neurofibromin, a large protein that functions as a negative regulator of Ras signaling and mediates pleiotropic cellular and organismal function. Recent evidence suggests NF1 may regulate metabolism, though the mechanisms are unknown. Here we show that the *Drosophila* ortholog of NF1, dNf1 regulates metabolic homeostasis in fruit flies by functioning within a discrete brain circuit. Loss of dNf1 increases metabolic rate and feeding, enhances starvation susceptibility, and decreases lipid stores while increasing lipid turnover rate. The increase in metabolic rate is independent of locomotor activity (grooming), and maps to a subset of neurons in the ventral nervous system. The feeding and metabolic rate effects are due to loss of dNf1 in the same set of neurons, suggesting that increased feeding may be a compensatory effect driven by the increase in metabolic rate and lipid turnover. Finally, we show that the Ras GAP-related domain of neurofibromin is required for normal metabolism, demonstrating that Ras signaling downstream of dNf1 mediates the metabolic effects. These data demonstrate that dNf1 regulates metabolic rate via neuronal mechanisms, suggest that cellular and systemic metabolic alterations may represent a pathophysiological mechanism in NF1, and provide a platform for investigating the cellular role of neurofibromin in metabolic homeostasis.

bioRxiv preprint doi: https://doi.org/10.1101/834788; this version posted November 8, 2019. The copyright holder for this preprint (which was not certified by peer review) is the author/funder. All rights reserved. No reuse allowed without permission.

INTRODUCTION

Neurofibromatosis type 1 (NF1) is a genetic disorder affecting 1 in ~3,500 individuals. Caused by mutations in the *NF1* gene, this disorder is characterized by benign tumors of the nervous system called neurofibromas, as well as an increased susceptibility to a range of complications including various cancers and neurocognitive deficits (e.g., attention-deficit/hyperactivity disorder, autism spectrum disorder, visuospatial memory impairments) (Diggs-Andrews and Gutmann, 2013; Hyman et al., 2005). The *NF1* tumor suppressor gene encodes a large protein called neurofibromin, which contains a central GAP-related domain (GRD) that enhances the GTPase activity of the small guanine nucleotide binding protein Ras, thereby down-regulating its biological activity (Cichowski and Jacks, 2001; Ratner and Miller, 2015). Ras, in turn, signals through multiple effectors, including mTOR, ERK, and, potentially cAMP/PKA indirectly (Gehart et al., 2010). Due to the numerous cellular functions of Ras, as well as potential interactions of neurofibromin with other signaling molecules (Ho et al., 2007; Ratner and Miller, 2015; Xie et al., 2016), loss of NF1 results in pleiotropic effects on cellular and organismal physiology which underlie this multisystem disorder. A major question is what are the central pathophysiological mechanism(s) of NF1; how does loss of NF1 alter cellular physiology resulting in cellular/behavioral phenotypes seen in NF1 patients and in animal models for the disease?

Emerging evidence suggests that NF1 regulates cellular and organismal metabolism. NF1 has been associated with short stature, as well as reduced body mass index in males (Koga et al., 2016; Souza et al., 2016), although the mechanisms underlying these manifestations are unknown. Alterations in certain metabolites have been reported in NF1 patients, though these are sex-specific (Koga et al., 2016). The incidence of diabetes mellitus, deaths from diabetes mellitus, and fasting blood glucose levels are lower in individuals with NF1 than in healthy controls (Martins et al., 2016). Of potential importance for NF1-associated tumorigenesis, loss

bioRxiv preprint doi: https://doi.org/10.1101/834788; this version posted November 8, 2019. The copyright holder for this preprint (which was not certified by peer review) is the author/funder. All rights reserved. No reuse allowed without permission.

of NF1 increases glycolysis and decreases respiration via Ras/ERK signaling in mitochondria (Masgras et al., 2017). Finally, increased resting energy expenditure has been reported in females with NF1 (Souza et al., 2019). Therefore, NF1 has the potential to regulate cellular and organismal metabolism, and alterations in metabolism may contribute to its pathophysiology. However, clinical studies have produced sometimes contradictory results across cohorts/sexes, often include low sample sizes, and the multisystemic nature of the disorder precludes identification of the mechanism(s) underlying the reported effects. Thus, the fundamental effects of NF1 on metabolism remain an open question.

We have investigated the role of the *Drosophila melanogaster* ortholog of NF1 (dNf1) in the regulation of metabolism. *Drosophila* neurofibromin is ~60% identical to the human protein and similarly mediates Ras signaling (The et al., 1997; Walker et al., 2013). Flies with *dNf1* mutations exhibit small body size (The et al., 1997; Walker et al., 2013; Walker et al., 2006), impaired circadian rhythms (Williams et al., 2001), learning and memory deficits (Buchanan and Davis, 2010; Gouzi et al., 2011; Guo et al., 2000), decreased lifespan via increased susceptibility to oxidative stress (Tong et al., 2007), and increased spontaneous grooming (King et al., 2016). These changes demonstrate widespread alterations in cellular/neuronal function, raising the possibility that metabolic alterations could be a central phenotype of NF1 deficiency across phyla.

bioRxiv preprint doi: https://doi.org/10.1101/834788; this version posted November 8, 2019. The copyright holder for this preprint (which was not certified by peer review) is the author/funder. All rights reserved. No reuse allowed without permission.

RESULTS

Loss of dNf1 increases metabolic rate via neuronal mechanisms

To test whether dNf1 affects metabolic rate, we examined CO_2 production via respirometry (Fig. 1A) (Yatsenko et al., 2014). In insects, whole body CO_2 production provides a readout of metabolic rate and can be readily measured in freely moving animals (Lighton, 2008). We first compared $Nf1^{P1}$ mutants, which harbor a large deletion in the *dNf1* locus, including the central catalytic GRD (The et al., 1997), with w^{CS10} controls. $Nf1^{P1}$ mutant adult flies exhibited significantly elevated CO_2 output compared to controls (Fig. 1B and S1A), suggesting that dNf1 plays a role in metabolic regulation. For additional confirmation, we tested a heteroallelic combination of the $Nf1^{P1}$ deletion with a nonsense mutation, $Nf1^{E1}$ (Walker et al., 2006). $Nf1^{P1/E1}$ mutants also exhibited significantly elevated CO_2 output relative to w^{CS10} control flies (Fig. 1C and S1B). To test whether the effect observed in *dNf1* mutants is localized to neurons, we knocked down dNf1 with RNAi using the Gal4/UAS system. In independent experiments, two different pan-neuronal Gal4 drivers were used to drive the RNAi: nSyb-Gal4 and R57C10-Gal4. In each case, a significant elevation in CO_2 production was observed in the experimental group relative to flies harboring either the heterozygous driver (Gal4/+) or effector (UAS/+) transgenes alone (Fig. 1D and S1C). This suggests that the loss of dNf1 function elevates metabolic rate via neuronal mechanisms.

To identify the neurons responsible for the increase in CO_2 production, we knocked down dNf1 using neuronal subset-selective Gal4 drivers. Drivers were selected that express in neurons that release particular neurotransmitters (e.g., cholinergic neurons [ChAT]), modulate growth and/or metabolism (e.g., insulin-like peptides [ILPs], c673a) (Al-Anzi et al., 2009), or mediate

bioRxiv preprint doi: https://doi.org/10.1101/834788; this version posted November 8, 2019. The copyright holder for this preprint (which was not certified by peer review) is the author/funder. All rights reserved. No reuse allowed without permission.

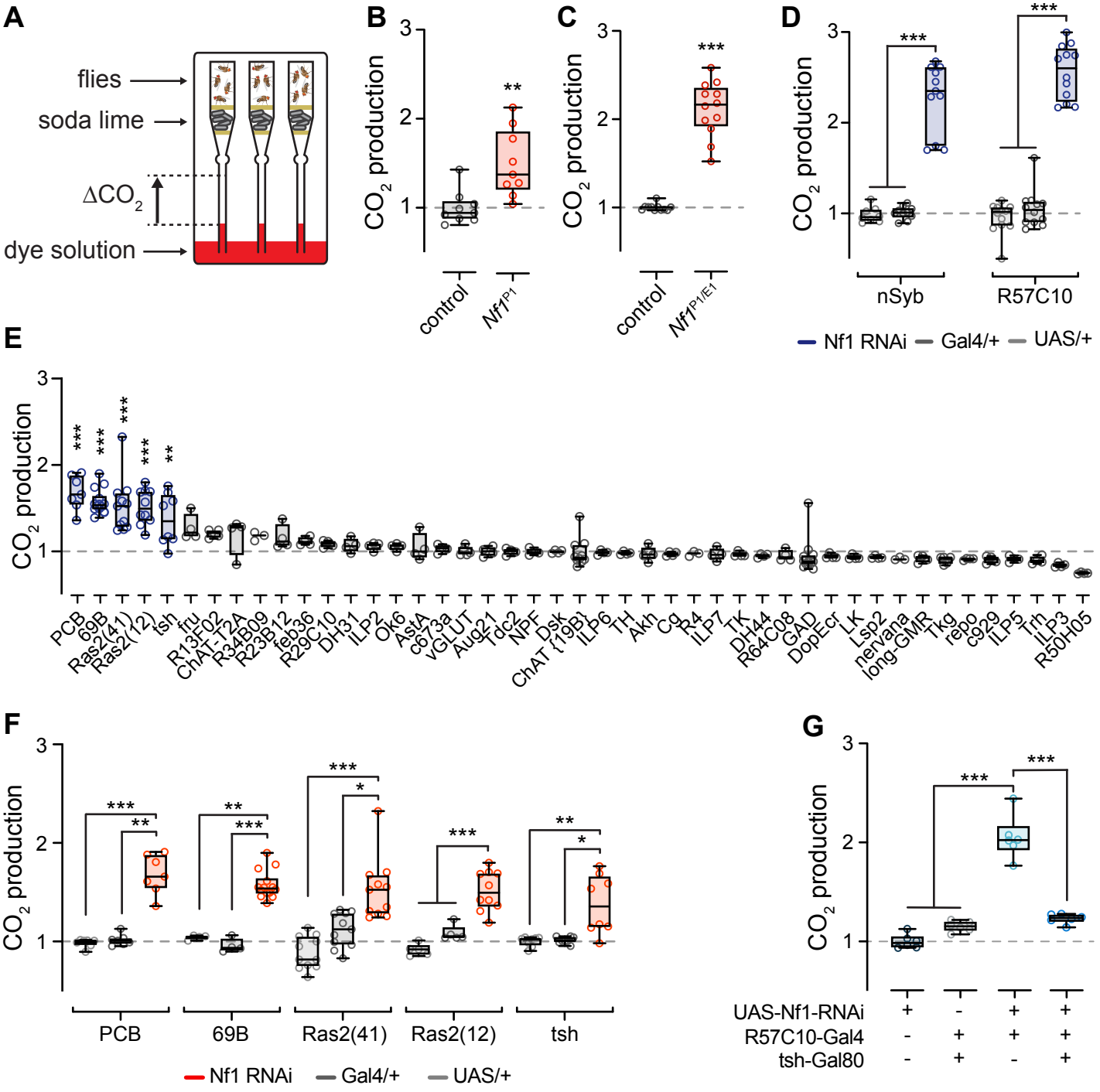

Figure 1. Loss of dNf1 increases CO_2 production via neuronal mechanisms. (A) Diagram of respirometry apparatus. (B) CO_2 production in *Nf1*^{P1} mutants and *w*^{CS10} controls, with mutants normalized to controls. **p < 0.01 (Mann-Whitney, n = 9). (C) Normalized CO_2 production in heteroallelic *Nf1*$^{P1/E1}$ mutants and matched genetic background controls. ***p < 0.001 (Mann-Whitney, n = 11-12). (D) CO_2 production when dNf1 was knocked down with RNAi driven by pan-neuronal Gal4 lines: nSyb- and R57C10-Gal4. Gal4/+ and UAS/+ are heterozygous controls. For each driver, data are normalized to the mean of both controls. ***p < 0.001 (Dunn's test, n = 8-12). (E) Screen for neuronal subsets in which knocking down dNf1 elevates CO_2 production. Normalized CO_2 production from each Gal4 line is shown. (F) Significant lines from panel E, showing both RNAi and heterozygous control groups. *p < 0.05, **p < 0.01, ***p < 0.001 (Dunn's test, n = 7-14). (G) Normalized CO_2production when knocking down dNf1 pan-neuronally with R57C10-Gal4, with and without the addition of the tsh-Gal80 repressor. ***p < 0.001 (Sidak, n = 6).

bioRxiv preprint doi: https://doi.org/10.1101/834788; this version posted November 8, 2019. The copyright holder for this preprint (which was not certified by peer review) is the author/funder. All rights reserved. No reuse allowed without permission.

previously characterized dNf1 effects on growth in larvae (e.g., Ras2) (Walker et al., 2006). For each line, the experimental group was compared to the two heterozygous genetic controls (Gal4/+ and UAS/+) within experiments. Among the 45 lines tested, 5 lines exhibited significant elevation of metabolic rate relative to both controls (Fig. 1 E,F and S1E). The positive lines were, in descending order of effect size, PCB, 69B, Ras2(41), Ras2(12), and tsh (Fig. 1F and S1E). The PCB-Gal4, described in more detail below, expresses in a sparse subset of neurons in the nervous system. The 69B and Ras2 drivers express broadly across the nervous system. Within neurons, the tsh-Gal4 line expresses preferentially in the ventral nervous system (VNS), suggesting that neurons in the VNS may be a major contributor to the metabolic phenotype. To further localize the effect, we parsed the brain and VNS with an intersectional approach. We drove the dNf1 RNAi pan-neuronally with R57C10 in one set of flies and suppressed VNS expression with the tsh-Gal80 repressor in another group (Fig. 1G and S1D). The tsh-Gal80 repressor differentially removes expression from neurons in the VNS (Clyne and Miesenbock, 2008). Limiting expression with tsh-Gal80 eliminated the metabolic phenotype, suggesting that dNf1-sensitive neurons are tsh-positive, and may reside in the VNS.

The mapping experiments revealed several major aspects of the dNf1-mediated neuronal control of metabolism. First, the dNf1 effect on metabolic rate was not due to the effects on a selective neurotransmitter system or neuronal subset (notably GABAergic and cholinergic neurons and neurons that release insulin-like peptides). Instead, knocking down dNf1 in relatively broader sets of neurons in the brain and/or VNS was required to drive an increase in metabolic rate. The driver with the most restricted expression pattern that produced a large effect was the PCB-Gal4 driver (Fig. 2A). This driver has a Gal4 enhancer trap in the pyruvate carboxylase (PCB) locus, and it has been previously termed “fatbody-Gal4” due to positive expression in the fat body (Gronke et al., 2003). However, our experiments suggest that the

bioRxiv preprint doi: https://doi.org/10.1101/834788; this version posted November 8, 2019. The copyright holder for this preprint (which was not certified by peer review) is the author/funder. All rights reserved. No reuse allowed without permission.

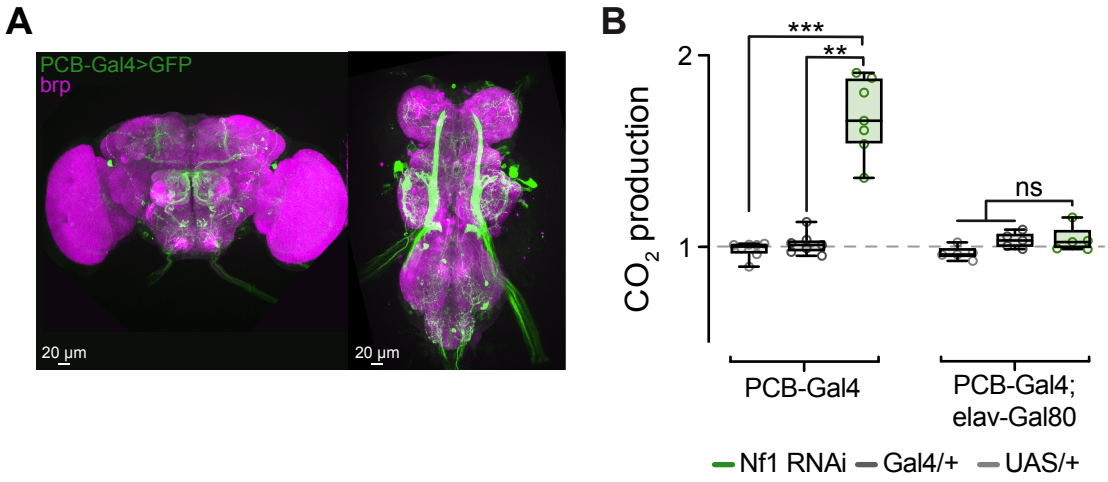

Figure 2. Knocking down dNf1 in a sparse set of neurons increases metabolic rate. (A) Expression of GFP (green) in neurons labeled by the PCB-Gal4 driver. Bruchpilot (brp) was used to counterstain neuropil (magenta). (B) CO_2 production assayed by respirometry. dNf1 was knocked down in neurons with the PCB-Gal4 driver, with or without the elav-Gal80 repressor. The PCB-Gal4 without Gal80 data set is the same as in Figure 1, shown here for comparison. ns: not significant. **p < 0.01 ***p < 0.001 (Dunn's test, n = 5-7).

bioRxiv preprint doi: https://doi.org/10.1101/834788; this version posted November 8, 2019. The copyright holder for this preprint (which was not certified by peer review) is the author/funder. All rights reserved. No reuse allowed without permission.

115 metabolic phenotype is neuronal in origin. Therefore, we tested whether this driver also exhibits
116 neuronal expression. Using the PCB-Gal4 to drive green fluorescent protein (mCD8::GFP, we
117 fixed and immunostained adult brains and VNS, and found sparse but robust GFP expression in
118 neurons in both regions (Fig. 2A). Given that the driver is not fat body-specific, we propose that
119 it be referred to by its genomic locus (PCB-Gal4) and do so here.

120

121 To further examine whether the metabolic effect was due to fat body or neuronal expression, we
122 tested three other fat body-expressing Gal4 drivers: R4, Cg and Lsp2. None of these produced
123 a metabolic phenotype when knocking down dNf1 (Figs. 1E, S2). In addition, we subtracted
124 neuronal expression from the PCB-Gal4 driver with elav-Gal80 (Yang et al., 2009) (Figs. 2B,
125 S3). This eliminated the dNf1-induced metabolic effect, providing additional evidence that
126 neurons in the PCB driver were responsible for the effect. Finally, 69B-Gal4, one of the Gal4
127 lines with largest effect sizes (Fig. 1 E,F), has previously been shown to be expressed in the
128 central nervous system but not in the fat body (Palgi et al., 2012). Thus, multiple lines of
129 evidence support the interpretation that neuronal expression in the PCB-Gal4 driver, rather than
130 fat body expression, is responsible for the metabolic phenotype. Overall, these data suggest
131 that dNf1 is required in a subset of neurons labeled by the PCB-Gal4 driver for normal metabolic
132 regulation.

133

134 To gain further insight into the mechanistic underpinnings of the metabolic phenotype, we
135 turned to stop-flow respirometry, quantifying O_2 consumed and CO_2 produced with stop-flow
136 respirometry (Fig. 3A) (Stahl et al., 2017). Mutant $Nf1^{P1}$ adult flies exhibited increased O_2
137 consumption and CO_2 production across the 24-hr photoperiod relative to controls (Fig. 3 B,D).
138 These differences were significant when the data were binned into both day and night periods

bioRxiv preprint doi: https://doi.org/10.1101/834788; this version posted November 8, 2019. The copyright holder for this preprint (which was not certified by peer review) is the author/funder. All rights reserved. No reuse allowed without permission.

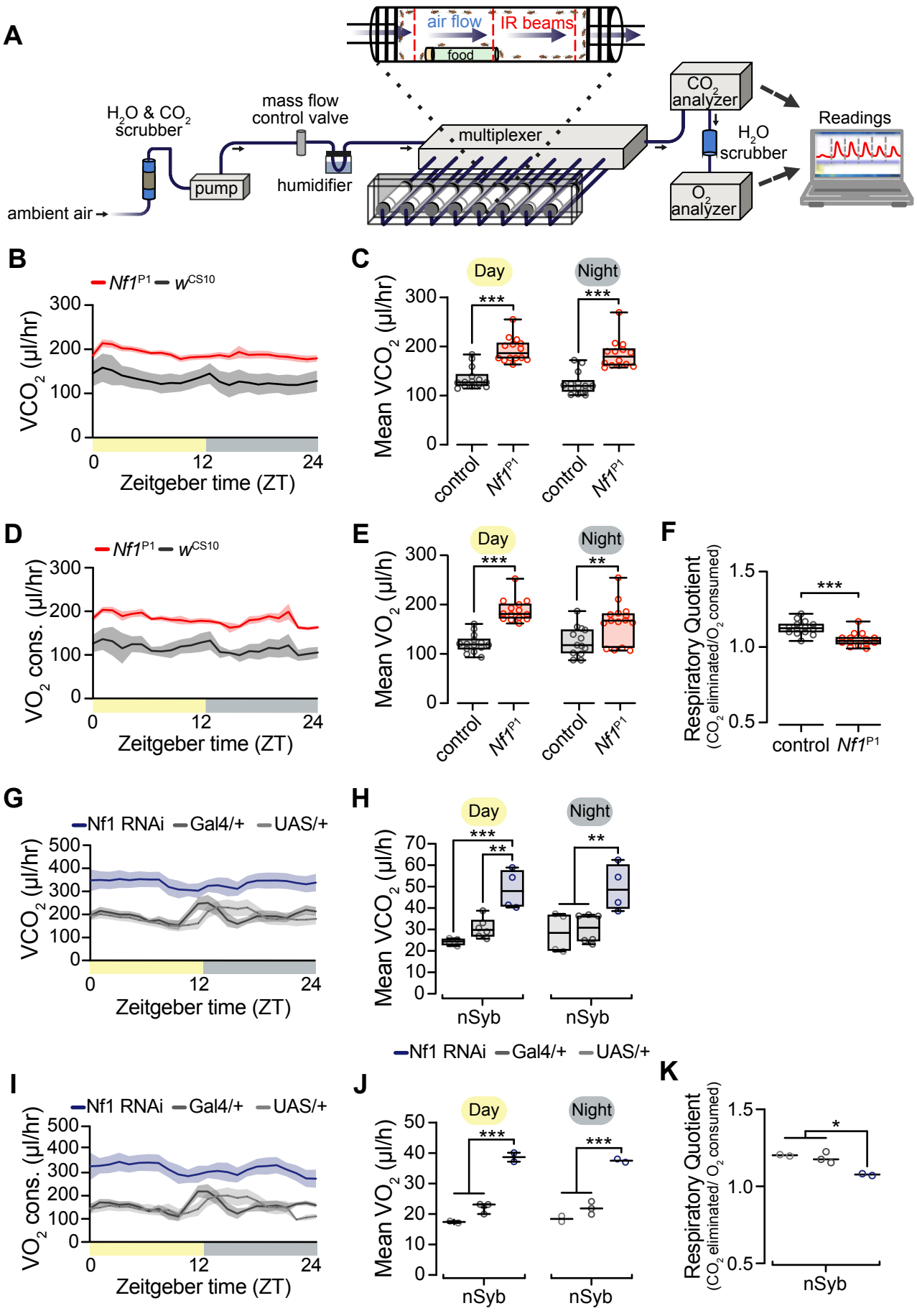

bioRxiv preprint doi: https://doi.org/10.1101/834788; this version posted November 8, 2019. The copyright holder for this preprint (which was not certified by peer review) is the author/funder. All rights reserved. No reuse allowed without permission.

Figure 3. Loss of dNf1 increases metabolic rate across the circadian photoperiod. (A) O_2 consumption and CO_2 production were measured with indirect calorimetry. (B) CO_2 production measured in *Nf1*^{P1} mutants and *w*^{CS10} controls, plotted in 1-hr bins across the circadian photoperiod. (C) Quantification of CO_2 production during day and night periods. ***p < 0.001 (Sidak, n = 14). (D) O_2 consumption measured in *Nf1*^{P1} mutants and *w*^{CS10} controls, plotted in 1-hr bins across the circadian photoperiod. (E) Quantification of O_2 consumption from panel D during day and night periods. **p < 0.01, ***p < 0.001 (Sidak, n = 13-15). (F) Respirometry quotient in *Nf1*^{P1} mutants and *w*^{CS10} controls. ***p < 0.001 (Mann-Whitney; n = 14). (G) CO_2 production, comparing pan-neuronal nSyb>RNAi with heterozygous controls, plotted in 1-hr bins across the circadian photoperiod. (H) Quantification of CO_2 production from panel G during day and night periods. **p < 0.01, ***p < 0.001 (Sidak, n = 4-6). (I) O_2 consumption, comparing pan-neuronal nSyb>RNAi lines with heterozygous controls, plotted in 1-hr bins across the circadian photoperiod. (J) Quantification of O_2 production from panel I during day and night periods. ***p < 0.001 (Sidak, n = 2-3). (K) Respirometry quotient in nSyb>RNAi lines and heterozygous controls. *p < 0.05 (Sidak, n = 2-3).

bioRxiv preprint doi: https://doi.org/10.1101/834788; this version posted November 8, 2019. The copyright holder for this preprint (which was not certified by peer review) is the author/funder. All rights reserved. No reuse allowed without permission.

(Fig. 3 C,E). Similarly, when dNf1 was knocked down pan-neuronally using nSyb-Gal4, we observed increased O_2 consumption and CO_2 production across the circadian photoperiod relative to controls (Fig. 3 G-J). In both cases, the respiratory quotient (RQ), the ratio of CO_2 eliminated to O_2 consumed, was significantly reduced in dNf1 loss of function (Fig. 3 F,K). Decreased RQ is consistent with increased utilization of endogenous fat stores (Stahl et al., 2017), suggesting that loss of dNf1 may increase fat utilization, a possibility we consider further below. Overall, these data provide independent support for the role of dNf1 in metabolic regulation, demonstrate that it is consistent across the 24-hr photoperiod, and suggest that it may result from altered fat homeostasis.

Metabolic regulation is independent of grooming

Loss of dNf1 increases spontaneous grooming (King et al., 2016), which could drive an increase in energy expenditure. To test whether this accounts for the increase in metabolic rate observed here, we knocked down dNf1 and quantified grooming in an open field arena (Fig. 4A). Pan-neuronal knockdown of dNf1 elevated spontaneous grooming (Fig. 4B), as previously reported (King et al., 2016). In addition, we tested the more restricted PCB-Gal4 driver. While knocking down dNf1 with this driver produced one of the largest increases in metabolic rate (Fig. 1 E,F), it did not significantly elevate spontaneous grooming (Fig. 4C). Therefore, dNf1 functions in independent populations of neurons to regulate metabolic rate and grooming. Further, these findings reveal that the elevated metabolic rate observed in *dNf1* mutant flies is not due to changes in grooming.

Loss of dNf1 increases starvation susceptibility by decreasing lipid stores via increased lipolysis

bioRxiv preprint doi: https://doi.org/10.1101/834788; this version posted November 8, 2019. The copyright holder for this preprint (which was not certified by peer review) is the author/funder. All rights reserved. No reuse allowed without permission.

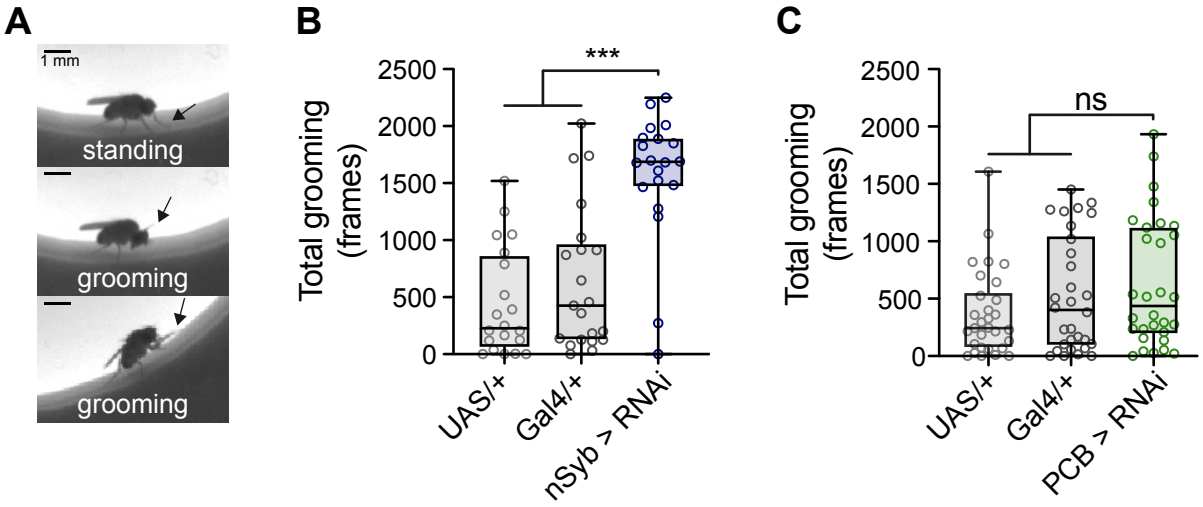

Figure 4. Knockdown of dNf1 in PCB-Gal4+ neurons does not affect spontaneous grooming. (A) Representative images of fly grooming in an open field. Top panel: a fly standing in place (not grooming). Middle panel: a fly grooming its head. Bottom panel: a fly grooming its prothoracic (front) legs. In all panels, an arrow points to the prothoracic leg location. Scale bars = 1mm. (B) Quantification of grooming in flies in which dNf1 has been knocked down pan-neuronally with the nSyb-Gal4 driver. $p < 0.001$ (Kruskal-Wallis), ***$p<0.001$ (Dunn; n = 20-21). (C) Quantification of grooming in flies in which dNf1 has been knocked down with the PCB-Gal4 driver. ns: not significant. $p = 0.209$ (Kruskal-Wallis, n = 30).

bioRxiv preprint doi: https://doi.org/10.1101/834788; this version posted November 8, 2019. The copyright holder for this preprint (which was not certified by peer review) is the author/funder. All rights reserved. No reuse allowed without permission.

Alterations in metabolic rate could be expected to affect lipid storage, and the decreased respirometry quotient suggests that lipid stores may be reduced. To directly test this, we first quantified triglyceride content using coupled colorimetry (Fig. 5A) (Tennessen et al., 2014). Triglyceride stores were significantly reduced in *dNf1* mutants compared to controls (Fig. 5A). Changes in either lipogenesis or lipolysis can decrease triglyceride levels (Fig. 5B). To determine which of these processed is dysregulated, we examined lipid turnover in a pulse-chase experiment (Fig. 5C). Flies were fed radiolabeled ^{14}C sucrose for 24 hr. Incorporation of ^{14}C sucrose into fatty acids in the flies was measured with scintillation at 0 hr or 48 hr after returning flies to normal, unlabeled food. Initial incorporation of ^{14}C did not differ between controls and $Nf1^{P1}$ mutants, suggesting that the synthesis of fatty acids (i.e., lipogenesis rate) was unchanged (Fig. 5D). However, after 48 hr, $Nf1^{P1}$ flies retained significantly less ^{14}C than controls, suggesting that the mutants exhibited increased rates of lipolysis. The effect was significant regardless of whether incorporation was normalized to body weight or the number of flies (data not shown). Together, these findings suggest that lipid levels are reduced in *dNf1* mutant flies due to increased lipolysis.

Triglycerides provide a major source of nutrients in flies that is critical for survival in nutrient-poor conditions. To determine whether the reduced triglyceride levels and increased metabolic rate impact survival in the absence of food, we measured the starvation resistance of $Nf1^{P1}$ mutants and controls flies. *dNf1* mutants were significantly more susceptible to starvation, succumbing in less than half the time of control flies when housed on a nutrient-free agar media (Fig. 5E). This suggests that loss of dNf1 increases starvation susceptibility, potentially due to the altered lipid homeostasis, which leaves the flies with lower reserves to draw on during caloric restriction.

bioRxiv preprint doi: https://doi.org/10.1101/834788; this version posted November 8, 2019. The copyright holder for this preprint (which was not certified by peer review) is the author/funder. All rights reserved. No reuse allowed without permission.

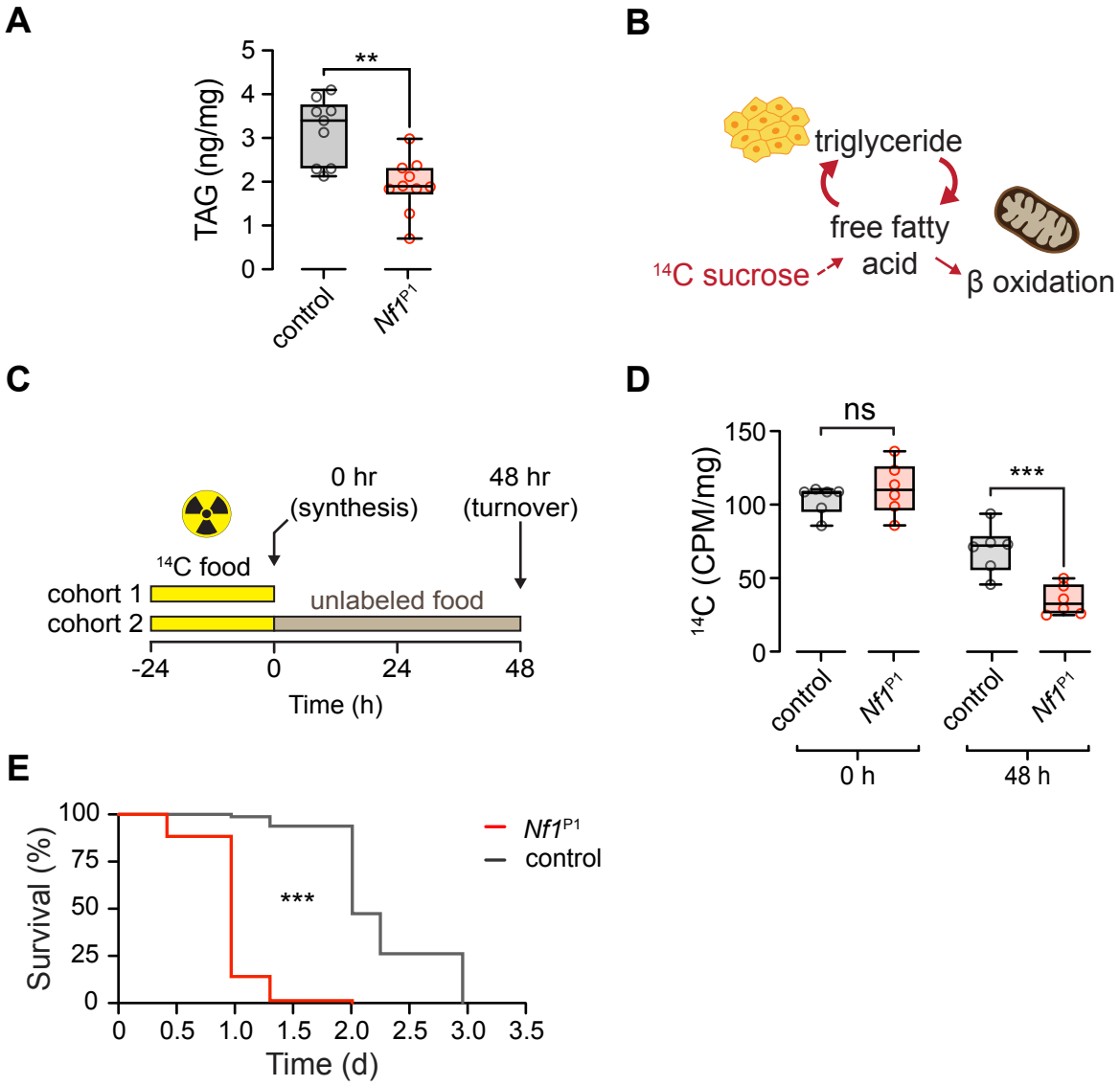

Figure 5. Loss of dNf1 reduces starvation resistance, decreases triglyceride levels, and increases lipid turnover rate. (A) Quantification of total body triglyceride (TAG) content in *Nf1*^{P1} mutants and w^{CS10} controls. **p < 0.01 (Mann-Whitney), n = 9-10. (B) Diagram of ^{14}C sucrose radiolabeling and lipid turnover. (C) Experimental protocol of ^{14}C sucrose radiolabeling protocol for lipid turnover analysis. (D) Quantification of lipid turnover via ^{14}C sucrose radiolabeling. Radioactivity was measured as counts per minute (CPM) and normalized to fly weight (mg). ns: not significant, ***p < 0.001 (Sidak; n = 6). (E) Lifespan under starvation, comparing *Nf1*^{P1} mutants (n = 78) and w^{CS10} controls (n = 80). *** p < 0.0001 ($X^2(1) = 154.0$, Mantel-Cox test).

bioRxiv preprint doi: https://doi.org/10.1101/834788; this version posted November 8, 2019. The copyright holder for this preprint (which was not certified by peer review) is the author/funder. All rights reserved. No reuse allowed without permission.

188 **Loss of dNf1 increases feeding in adult flies**

189 Feeding and energy stores are homeostatically regulated, and animals often compensate for
190 depleted energy stores by increasing food intake. Since loss of dNf1 increased metabolic rate,
191 decreased lipid stores, and increased lipid turnover via increased lipolysis, energy intake could
192 be increased as a homeostatic compensatory mechanism. To test this, we examined feeding
193 using a capillary feeding assay (Murphy et al., 2017) (Fig. 6A). Food intake was significantly
194 increased in $Nf1^{P1}$ adult flies relative to controls (Fig. 6B). Knocking down dNf1 pan-neuronally
195 also increased feeding relative to controls (Fig. 6C), confirming the effect and suggesting that it
196 was due to the loss of dNf1 specifically in neurons. We next tested the neuronal circuit
197 requirements for dNf1 in the context of feeding. A selection of Gal4 drivers that labeled different
198 neurochemical subsets, and/or produced metabolic alterations, were used to drive dNf1 RNAi
199 (Fig. 6D). Among these lines, significant elevations in feeding were observed when dNf1 was
200 knocked down pan-neuronally (nSyb), selectively in the VNS (tsh), and in subsets of neurons
201 labeled by the 69B and PCB-Gal4 drivers. No effect was observed when dNf1 was knocked
202 down in GABAergic neurons (GAD) or insulin-like peptides (ILP2, ILP3, ILP5, ILP 6, ILP7) (Fig.
203 6D). Thus, knocking down dNf1 in the same circuits that elevated metabolic rate (Fig. 1 E,F)
204 also drove an increase in feeding. While it is possible that dNf1 independently regulates both
205 phenotypes via actions in the same circuit(s), we surmise that the increase in feeding is likely a
206 homeostatic response to the increase in metabolic rate and decrease in fat stores caused by
207 loss of dNf1.

208

209 **Ras GAP-related domain signaling underlies the Nf1 metabolic alterations**

210 While the catalytic RasGAP activity of neurofibromin is located in its central portion, the GRD,
211 other parts of the protein may contain other functions that could mediate cellular effects

bioRxiv preprint doi: https://doi.org/10.1101/834788; this version posted November 8, 2019. The copyright holder for this preprint (which was not certified by peer review) is the author/funder. All rights reserved. No reuse allowed without permission.

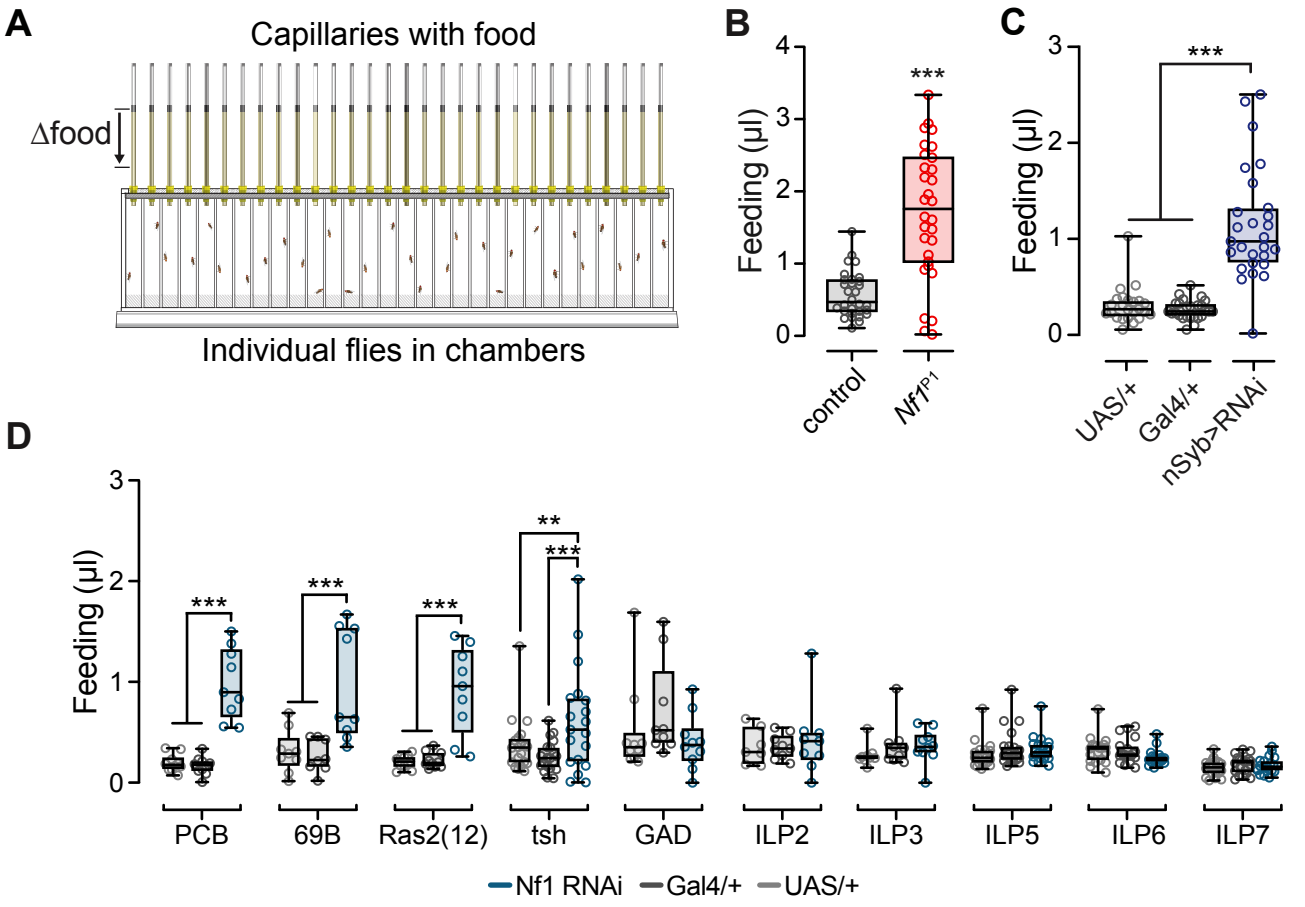

Figure 6. Loss of dNf1 increases feeding. (A) Illustration of the capillary feeding apparatus. (B) Feeding in *Nf1*^{P1} mutants and *w*^{CS10} controls. ***p < 0.001 (Mann-Whitney, n = 30) (C) Feeding with pan-neuronal dNf1 RNAi (driven by nSyb-Gal4) and heterozygous Gal4/+ and UAS/+ controls. ***p < 0.001 (Dunn's test, n = 24-27) (D) Feeding measured with knockdown of dNf1 in different subsets of neurons with various Gal4 drivers. *p < 0.05, **p < 0.01, ***p < 0.001 (Dunn's test, n = 7-20).

bioRxiv preprint doi: https://doi.org/10.1101/834788; this version posted November 8, 2019. The copyright holder for this preprint (which was not certified by peer review) is the author/funder. All rights reserved. No reuse allowed without permission.

(Cichowski and Jacks, 2001; Ratner and Miller, 2015). To determine the critical cellular signaling pathway(s) mediating dNf1 effects on metabolic rate, we first tested the role of the GRD. We utilized the UAS/Gal4 system to express dNf1 in flies with the heteroallelic $Nf1^{P1/E1}$ mutant combination. Pan-neuronal rescue of full-length, wild-type dNf1 restored metabolic rate to control levels (Fig. 7 A,B). In contrast, pan-neuronal expression of full-length dNf1 carrying a missense mutation in the "arginine finger" of the GRD, R1320P, did not rescue the metabolic effect (Fig. 7 A,B). This mutation corresponds to the patient-derived R1276P mutation in *NF1* shown to reduce Ras GAP activity >1000 fold (Klose et al., 1998; Walker et al., 2006). These data suggest that expression of wild-type dNf1 in neurons restores normal metabolic rate and that RasGAP activity is necessary for dNf1 metabolic effects.

DISCUSSION

This study provides insight into the role of dNf1 in regulating basal metabolic rate via neuronal mechanisms in *Drosophila*. The data support the following major specific conclusions about the role of dNf1 in regulating metabolic rate: 1) loss of dNf1 increases metabolic rate, independent of locomotor changes (grooming), 2) loss of dNf1 function decreases fat stores via increased lipolysis, while increasing food consumption, 3) dNf1 modulates metabolism via a subset of neurons in the VNS labeled by the PCB-Gal4 driver, and 4) dNf1 acts via the GRD to alter metabolic function.

We found that dNf1 plays a central role in regulating metabolic rate via both indirect and stop-flow respirometry. Null genomic mutations and pan-neuronal RNAi knockdown of dNf1 caused significant elevations in metabolic rate. We tested multiple driver lines to determine which cell types are most affected by dNf1 loss of function, finding that dNf1 acts on a relatively narrow set

bioRxiv preprint doi: https://doi.org/10.1101/834788; this version posted November 8, 2019. The copyright holder for this preprint (which was not certified by peer review) is the author/funder. All rights reserved. No reuse allowed without permission.

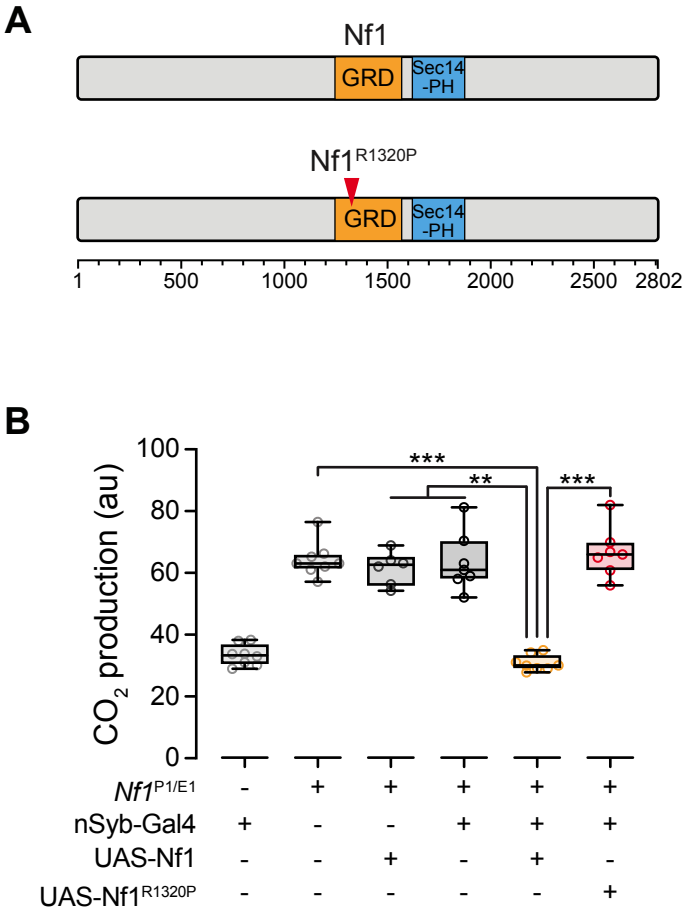

Figure 7. dNf1 metabolic effects are rescued by full-length dNf1 and require a functional GAP-related domain. (A) Major domains in neurofibromin and the site of the R1320P mutation. GRD: GAP-related domain, PH: pleckstrin homology-like domain. (B) Transgenic expression of full-length dNf1 and dNf1^{R1320P} in the heteroallelic *Nf1*$^{P1/E1}$ mutant background. Full length dNf1 rescues CO_2 production to nSyb-Gal4/+ levels. **p < 0.01 ***p < 0.001 (Dunn's test, n = 6-8). au: arbitrary units.

bioRxiv preprint doi: https://doi.org/10.1101/834788; this version posted November 8, 2019. The copyright holder for this preprint (which was not certified by peer review) is the author/funder. All rights reserved. No reuse allowed without permission.

of neurons to modulate metabolic rate. These neurons were not ones commonly implicated in metabolism, feeding, or organismal growth, as knocking down dNf1 in insulin-producing cells, peptidergic neurons, ring gland cells, monoaminergic neurons, etc., produced no effect. It was particularly surprising that loss of dNf1 function in the insulin-producing cells yielded no significant changes in metabolism or feeding, as the insulin-like peptides released by these neurons are functional homologs of insulin and insulin-like growth factors. Furthermore, alterations to such cells affect starvation response and lipid stores (Baker and Thummel, 2007).

A sparse set of neurons in the nervous system, labeled most discretely by the PCB-Gal4 driver, was responsible for the dNf1 effect on metabolism. Due to additional fat body expression with this driver, we verified that the metabolic phenotype was due to loss of neuronal dNf1, using additional Gal4 lines that express in the adult and larval fat body. The fat body serves an important homeostatic function by storing lipids, similarly to white adipose tissue in mammals, and plays a role in the regulation of peripheral tissues under both fed and starved conditions (Baker and Thummel, 2007). Therefore, the lack of metabolic effects with multiple fat body specific drivers was notable. The effects of dNf1 on metabolic rate could theoretically be due to altered energy expenditure within neurons themselves or central control of metabolism. Our experiments implicate the latter, as the PCB-Gal4 driver labels a sparse neuronal population and drives a robust metabolic effect when used to knock down dNf1.

A previous study from our group observed increased grooming activity in *dNf1* mutants and with pan-neuronal RNAi. Increased locomotor activity, including activity such as grooming, might be expected to drive increases in metabolism. However, the dNf1 metabolic and grooming phenotypes were dissociable with the PCB-Gal4 driver, which increased metabolic rate without

bioRxiv preprint doi: https://doi.org/10.1101/834788; this version posted November 8, 2019. The copyright holder for this preprint (which was not certified by peer review) is the author/funder. All rights reserved. No reuse allowed without permission.

increasing grooming. Thus, we surmise that the effects of dNf1 on grooming and metabolic rate are caused by distinct neuronal circuits, with relatively little overlap. A thorough analysis of the neuronal circuit driving both phenotypes (particularly grooming) will be necessary to understand how dNf1 independently modulates these behaviors.

The metabolic effects we observed in the *Drosophila* model, combined with the conserved signaling and cellular functionality, suggest that loss of dNf1 could produce metabolic alterations across taxa. Ras is upstream of multiple signaling cascades that influence cellular metabolism, including mTOR, and ERK. mTOR and ERK are key metabolic regulators, exerting effects on gluconeogenesis, protein synthesis, adipocyte differentiation, lipid/cholesterol homeostasis, lipogenesis, and lipolysis (Gehart et al., 2010). Conditional knockout of dNf1 in mouse models, while rapidly lethal, produces metabolic alterations in muscle, including increased triglyceride content and activities of oxidative metabolism enzymes (Sullivan et al., 2014). Further, mouse embryonic fibroblasts lacking dNf1 show changes in basal metabolic rate and mitochondrial bioenergetics (Masgras et al., 2017). These findings, along with data from the present study, suggest the potential for homeostatic regulation of metabolic rate via dNf1-mediated mechanisms.

The most well-characterized biochemical function of neurofibromin is its RasGAP activity contained within the GRD. In the present experiments, transgenic expression of full-length, wild-type neurofibromin restored normal metabolic rate in *dNf1* mutants. However, expression of a dNf1 transgene containing the catalytically dead R1320P mutation failed to rescue. This mutation recapitulates the human patient-derived R1276P mutation that impacts the arginine finger of the GRD, reducing RasGAP activity >1000 fold (Klose et al., 1998). In addition to the

bioRxiv preprint doi: https://doi.org/10.1101/834788; this version posted November 8, 2019. The copyright holder for this preprint (which was not certified by peer review) is the author/funder. All rights reserved. No reuse allowed without permission.

GRD, neurofibromin contains other domains with potential functional significance, such as a lipid-binding pleckstrin-homology domain (Fig. 7). Thus, this experiment demonstrated that catalytic activity from the GRD itself was critical for dNf1 modulation of metabolic rate, rather than other putative functions such as lipid binding. Some studies have implicated Ras/GRD function in driving dNf1 phenotypes (Costa et al., 2002; Walker et al., 2006; Williams et al., 2001), while others have identified other signaling roles, for instance on dopaminergic signaling, G protein signal transduction, and cAMP signaling (Brown et al., 2010; Dasgupta et al., 2003; Diggs-Andrews et al., 2013; The et al., 1997; Walker et al., 2013; Wolman et al., 2014; Xie et al., 2016). Our data suggest that the GRD is necessary for dNf1-dependent modulation of metabolic rate, thereby implicating neuronal Ras signaling. The effects of aberrant Ras signaling could include transcriptional regulation, as Ras regulates the activity of multiple transcription factors (Masgras et al., 2017). Further, alterations in these signaling cascades may affect the release of neurotransmitters in ways that produce non-cell-autonomous effects on signaling cascades in other cells (Walker et al., 2006).

Among individuals with NF1, there are subtle alterations in growth, particularly reduced stature (Soucy et al., 2013), as well as reduced body mass index in males (Koga et al., 2016). Alterations in specific metabolites have been reported, though these are sex-specific (Koga et al., 2016). Diabetes mellitus – as well as deaths from noted diabetes complications – is rare in patients with NF1 (Koga et al., 2016). Loss of NF1 increases glycolysis and decreases respiration via mitochondrial ERK signaling, which may play a role in tumor growth (Masgras et al., 2017). Finally, increased resting energy expenditure was recently reported in a cohort of female NF1 patients as well as a decrease in respiratory quotient compared to healthy controls (Souza et al., 2019). Therefore, NF1 has the potential to regulate cellular and organismal metabolism, and alterations in metabolism may contribute to the pathophysiology of NF1. Our

bioRxiv preprint doi: https://doi.org/10.1101/834788; this version posted November 8, 2019. The copyright holder for this preprint (which was not certified by peer review) is the author/funder. All rights reserved. No reuse allowed without permission.

data suggest that changes in neuronal metabolic control may be a feature of the cellular and organismal alterations that occur following loss of dNf1.

ACKNOWLEDGMENTS

We thank Dr. Norbert Perrimon for Tk-gut-Gal4, Dr. Yuh-Nung Jan for lLP7-Gal4 and elav-Gal80, and Dr. Toshihiro Kitamoto for DopEcr-Gal4. Fly stocks obtained from the Bloomington Drosophila Stock Center (BDSC) (NIH P40OD018537) and from the Vienna Drosophila Resource Center (VDRC) were used in this study. Research support was provided by NIH R01 NS097237 (S.M.T), NIH R01 AG045036 (W.W.J.), NIH R01 NS085152 and DC017390 (A.C.K.), and NIH R21 NS096402 and DOD-NFRP W81XWH-16-1-0220 (J.A.W.).

AUTHOR CONTRIBUTIONS

S.M.T. provided overall project management and funding acquisition. S.M.T. and V.B. designed the project and drafted the manuscript. The manuscript was reviewed and edited by V.B., S.M.T., A.C.K., J.A.W., K.J.C., W.W.J, T.B., B.A.S., E.C.G., and K.R.M. Experimental methodology was performed by V.B., W.W.J., A.C.K., and K.J.C. Experiments were performed by V.B., B.A.S., K.R.M., E.C.G., T.B., S.P., L.B.K., and W.W.J. Project resources were provided by S.M.T., W.W.J., A.C.K., J.A.W., and K.J.C. Experimental and project supervision was provided by S.M.T., W.W.J., A.C.K., K.J.C., and L.B.K.

COMPETING INTERESTS

The authors declare no competing interests.

bioRxiv preprint doi: https://doi.org/10.1101/834788; this version posted November 8, 2019. The copyright holder for this preprint (which was not certified by peer review) is the author/funder. All rights reserved. No reuse allowed without permission.

METHODS

Drosophila Husbandry and Stocks

Flies were cultured on cornmeal/agar food medium according to standard protocol and housed at 25 ºC, 60% relative humidity, on a 12:12 light:dark cycle. The $Nf1^{P1}$ mutation was backcrossed six generations into the w^{CS10} genetic background and w^{CS10} flies were used as controls. Genetic control for $Nf1^{P1}/Nf1^{E1}$ trans-heterozygotes is $w^{CS10}/w^{iso2;3}$. UAS-dNf1-eGFP transgenes were generated using a *dNf1* mini-gene (full-length *dNf1* cDNA corresponding to the RF isoform with addition of introns 9 and 10). The R1320P mutation was created in a wild-type cDNA using the Q5 Site-Directed Mutagenesis Kit (New England Biolabs). Wild-type and R1320P mutant *dNf1* were then subcloned into the pUAST-attB vector with an in-frame C-terminal fusion with eGFP cDNA. Transgenic lines were produced by integrating the constructs at the attp40 site (Rainbow Transgenic Flies Inc.) The dNf1 RNAi line was obtained from the Vienna Drosophila RNAi Center (VDRC #109637), Gal4/+ control crosses consisted of an empty attP control line (VDRC #60100). UAS-dicer2 was included to potentiate the RNAi effect (Dietzl et al., 2007), and was included with the UAS-RNAi (i.e., all experimental and UAS/+ genotypes). Male flies were used for all experiments to prevent egg accumulation in behavioral chambers.

CO_2 measurement using respirometry

Respirometers were prepared as previously described (Yatsenko et al., 2014). Briefly, a 1 ml pipette tip and 50µl capillary micropipette were securely glued together. Soda lime was placed into each pipette tip between two foam pieces to avoid contact with flies. 16 respirometers were hung on a custom-made rack in a latch-lid measurement chamber. Flies were anesthetized with

bioRxiv preprint doi: https://doi.org/10.1101/834788; this version posted November 8, 2019. The copyright holder for this preprint (which was not certified by peer review) is the author/funder. All rights reserved. No reuse allowed without permission.

355 CO_2 and allowed to recover for at least 24 hr before beginning the experiment. Four flies of the
356 same genotype were placed into each pipette using an aspirator and tightly sealed at the top
357 using non-hardening modeling clay. One pipette was left empty in each chamber as a
358 temperature and atmospheric control. The measuring chamber was filled with 500mL red-dye
359 solution made with water-based dye. The latch-lid chamber with flies were left to equilibrate to
360 incubator conditions (25 ºC) for 1 hr before starting the experiment. Vacuum grease was applied
361 between the latch-lid and chamber to reduce atmospheric and temperature fluctuations. Images
362 were captured every 15 minutes using a time-lapse image software (PhenoCapture) and
363 analyzed using Fiji, measuring the liquid meniscus position in each capillary. This measurement
364 was subtracted from a reference image and repeated at each time point for 3 hr.

365

366 **Indirect calorimetry**

367 Metabolic rate was measured using the Sleep and Activity Metabolic Monitor (SAMM) system at
368 25 ºC through indirect calorimetry using a stop-flow, push-through respirometry system (Sable
369 Systems International). Metabolic rate in group-housed adult flies was measured as previously
370 described (Stahl et al., 2018; Stahl et al., 2017). Briefly, the experimental system assessed
371 baseline CO_2 levels from an empty chamber to measure CO_2 production and O_2 consumption
372 from 25 male adult flies. Air was flushed from each chamber for 50 sec to provide a readout of
373 CO_2 accumulation and O_2 consumption over a 10-min period. A H_2O and CO_2 scrubber was
374 used to dehumidify and remove CO_2 from air before being pumped into a mass flow control
375 valve to maintain a consistent flow rate. The air was then re-humidified by passing through a
376 reservoir containing deionized water prior to reaching the behavioral chambers. Each behavioral
377 chamber (70 mm long x 20 mm diameter glass tube) contained 25 adult male flies with a food
378 vial containing 1% agar and 5% sucrose. Flies were allowed to acclimate to system for 24 hr
379 before the start of each experiment. All experimental runs included a food-only control baseline

bioRxiv preprint doi: https://doi.org/10.1101/834788; this version posted November 8, 2019. The copyright holder for this preprint (which was not certified by peer review) is the author/funder. All rights reserved. No reuse allowed without permission.

chamber. CO_2 production was analyzed using a LI-7000 CO_2/H_2O Analyzer (LI-COR) and then dehumidified using a H_2O scrubber before O_2 consumption was measured Oxilla Dual Absolute Differential Oxygen Analyzer (LI-COR). CO_2 production and O_2 consumption recordings were taken every 10 min. Respirometry quotient (RQ) was calculated as volume of CO_2 eliminated/O_2 consumed.

Immunohistochemistry

Five to seven-day old PCB-Gal4 adult nervous systems were dissected in 1% paraformaldehyde in S2 medium and processed as previously described (Jenett et al., 2012). Samples were stained with primary antibodies for 3 hr at room temperature and at 4 ºC overnight, followed by secondary antibodies for 3 hr at room temperature and 4 d at 4 ºC. Incubations were performed in blocking serum (3% normal goat serum). Samples were mounted in Vectashield (Vector Laboratories) for analysis. The following antibodies were used: rabbit anti-GFP (1:1000, Invitrogen), mouse anti-nc82 (1:50, DSHB), goat anti-rabbit IgG and goat anti-mouse IgG (1:800, Alexa 488 or Alexa 633 respectively, Invitrogen). Leica TCS SP8 confocal microscopes were used to obtain images.

Total Grooming

Four to six-day old PCB-Gal4 adult males were used to measure total grooming, as previously described (King et al., 2016). Briefly, individual animals were aspirated into an open field area, habituated for 15 min, and a 5-min video recording was recorded for analysis. Videos were manually scored and start and stop frames were recorded for each grooming event. Total grooming was calculated as the sum of all grooming during the 5-min video.

bioRxiv preprint doi: https://doi.org/10.1101/834788; this version posted November 8, 2019. The copyright holder for this preprint (which was not certified by peer review) is the author/funder. All rights reserved. No reuse allowed without permission.

403

404 **Starvation survival**

405 Adult male flies (group housed, 20 flies/vial) on 1% (non-nutritional) agar. The percentage of
406 flies alive was measured twice every 24 hrs.

407

408 **Coupled colorimetric assay for TAG**

409 Five male adult w^{CS10} and $Nf1^{P1}$ were collected per sample, as previously described (Tennessen
410 et al., 2014). Samples were rinsed in PBS, rapidly homogenized in PBST, and the supernatant
411 was heated at 70 ºC for 10 min. The glycerol standard solution (Sigma 2.5 mg/ml triolein
412 equivalent glycerol standard; G7793) was prepared in PBST to generate 0.125, 0.25, and 0.5
413 mg/ml glycerol standards. Glycerol standards, samples and a PBST blank were then added to
414 two microfuge tubes and the triglyceride reagent (Sigma; T2449) was added to one of the two
415 tubes to free the glycerol backbone. All microfuge tubes were incubated at 37 ºC for 60 min.
416 Samples were transferred to a clear, flat bottom 96-well plate and free glycerol reagent (Sigma;
417 F6428) was added to each sample and mixed well. The plate was incubated for 5 min at 37 ºC
418 and centrifuged in a swing-bucket rotor. Absorbance was measured at 540 nm. TAG
419 concentration per sample was determined by subtracting the absorbance for the free glycerol in
420 untreated samples from the total glycerol concentration in samples with the triglyceride reagent
421 and then normalized by sample weight. TAG content in each sample is based on the triolein-
422 equivalent standard curve.

423

424 **Lipid Analysis**

bioRxiv preprint doi: https://doi.org/10.1101/834788; this version posted November 8, 2019. The copyright holder for this preprint (which was not certified by peer review) is the author/funder. All rights reserved. No reuse allowed without permission.

As described (Katewa et al., 2012), lipogenesis and lipolysis were measured in adult flies. Briefly, flies were fed with 5 µCi of ^{14}C- sucrose incorporated into standard fly food for 24 hr. After 24 hr, half of the flies were collected and frozen at -80 ºC to measure lipogenesis (0 h samples). The remaining flies were transferred to unlabeled standard fly food for 48 hr and then immediately frozen at -80 ºC to measure lipolysis (48 h samples). All flies were transferred into pre-weighed 1.7 ml Eppendorf tubes and then weighed to obtain fly mass. Frozen samples were homogenized with 200 µl of 2:1 chloroform: methanol mix for 15 minutes at room temperature and then spun at full speed for 15 minutes at room temperature. The supernatant was recovered and 40 µl of 0.9% (w/v) of NaCl was added. Samples were vortexed and spun gently to separate phases. The upper phase was removed, and the interphase was rinsed twice with 200 µl 1:1 methanol: water solution without mixing. The lower chloroform phase was used for scintillation counting.

Feeding

Feeding was quantified in adult male flies using a capillary feeding assay, as previously described (Ja et al., 2007). Briefly, individual flies were placed into chambers (46 mm x 7 mm) containing 1% agar at the bottom and a glass capillary at the top. Each glass capillary contained a meniscus labeling dye to track food consumption and an aqueous food solution (2.5% sucrose + 2.5% yeast extract). All flies were habituated to the chamber and liquid diet 72 hr before measuring food intake (glass capillaries were replaced daily). Total feeding was measured over 24 hr and analyzed by Noah.py (Murphy et al., 2017).

Statistical Analysis

bioRxiv preprint doi: https://doi.org/10.1101/834788; this version posted November 8, 2019. The copyright holder for this preprint (which was not certified by peer review) is the author/funder. All rights reserved. No reuse allowed without permission.

Normality of data was assessed with the D'Agostino-Pearson Test. Hypothesis testing was carried out with Student's t (parametric), one/two-way ANOVA with post-hoc Sidak (parametric), Mann-Whitney (nonparametric), Kruskal-Wallis with post-hoc Dunn (nonparametric), or Kaplan-Meier with Mantel-Cox (Log-rank) tests. All statistical analyses were performed using GraphPad Prism 8.1.2.

bioRxiv preprint doi: https://doi.org/10.1101/834788; this version posted November 8, 2019. The copyright holder for this preprint (which was not certified by peer review) is the author/funder. All rights reserved. No reuse allowed without permission.

REFERENCES

Al-Anzi, B., Sapin, V., Waters, C., Zinn, K., Wyman, R.J., and Benzer, S. (2009). Obesity-blocking neurons in Drosophila. Neuron 63, 329-341.

Baker, K.D., and Thummel, C.S. (2007). Diabetic larvae and obese flies-emerging studies of metabolism in Drosophila. Cell Metab 6, 257-266.

Brown, J.A., Gianino, S.M., and Gutmann, D.H. (2010). Defective cAMP generation underlies the sensitivity of CNS neurons to neurofibromatosis-1 heterozygosity. J Neurosci 30, 5579-5589.

Buchanan, M.E., and Davis, R.L. (2010). A distinct set of Drosophila brain neurons required for neurofibromatosis type 1-dependent learning and memory. J Neurosci 30, 10135-10143.

Cichowski, K., and Jacks, T. (2001). NF1 tumor suppressor gene function: narrowing the GAP. Cell 104, 593-604.

Clyne, J.D., and Miesenbock, G. (2008). Sex-specific control and tuning of the pattern generator for courtship song in Drosophila. Cell 133, 354-363.

Costa, R.M., Federov, N.B., Kogan, J.H., Murphy, G.G., Stern, J., Ohno, M., Kucherlapati, R., Jacks, T., and Silva, A.J. (2002). Mechanism for the learning deficits in a mouse model of neurofibromatosis type 1. Nature 415, 526-530.

Dasgupta, B., Dugan, L.L., and Gutmann, D.H. (2003). The neurofibromatosis 1 gene product neurofibromin regulates pituitary adenylate cyclase-activating polypeptide-mediated signaling in astrocytes. J Neurosci 23, 8949-8954.

Dietzl, G., Chen, D., Schnorrer, F., Su, K.C., Barinova, Y., Fellner, M., Gasser, B., Kinsey, K., Oppel, S., Scheiblauer, S*., et al.* (2007). A genome-wide transgenic RNAi library for conditional gene inactivation in Drosophila. Nature 448, 151-156.

Diggs-Andrews, K.A., and Gutmann, D.H. (2013). Modeling cognitive dysfunction in neurofibromatosis-1. Trends Neurosci 36, 237-247.

Diggs-Andrews, K.A., Tokuda, K., Izumi, Y., Zorumski, C.F., Wozniak, D.F., and Gutmann, D.H. (2013). Dopamine deficiency underlies learning deficits in neurofibromatosis-1 mice. Ann Neurol 73, 309-315.

Gehart, H., Kumpf, S., Ittner, A., and Ricci, R. (2010). MAPK signalling in cellular metabolism: stress or wellness? EMBO Rep 11, 834-840.

Gouzi, J.Y., Moressis, A., Walker, J.A., Apostolopoulou, A.A., Palmer, R.H., Bernards, A., and Skoulakis, E.M. (2011). The receptor tyrosine kinase Alk controls neurofibromin functions in Drosophila growth and learning. PLoS Genet 7, e1002281.

Gronke, S., Beller, M., Fellert, S., Ramakrishnan, H., Jackle, H., and Kuhnlein, R.P. (2003). Control of fat storage by a Drosophila PAT domain protein. Curr Biol 13, 603-606.

Guo, H.F., Tong, J., Hannan, F., Luo, L., and Zhong, Y. (2000). A neurofibromatosis-1-regulated pathway is required for learning in Drosophila. Nature 403, 895-898.

Ho, I.S., Hannan, F., Guo, H.F., Hakker, I., and Zhong, Y. (2007). Distinct functional domains of neurofibromatosis type 1 regulate immediate versus long-term memory formation. J Neurosci 27, 6852-6857.

Hyman, S.L., Shores, A., and North, K.N. (2005). The nature and frequency of cognitive deficits in children with neurofibromatosis type 1. Neurology 65, 1037-1044.

Ja, W.W., Carvalho, G.B., Mak, E.M., de la Rosa, N.N., Fang, A.Y., Liong, J.C., Brummel, T., and Benzer, S. (2007). Prandiology of Drosophila and the CAFE assay. Proc Natl Acad Sci U S A 104, 8253-8256.

Jenett, A., Rubin, G.M., Ngo, T.T., Shepherd, D., Murphy, C., Dionne, H., Pfeiffer, B.D., Cavallaro, A., Hall, D., Jeter, J*., et al.* (2012). A GAL4-driver line resource for Drosophila neurobiology. Cell Rep 2, 991-1001.

King, L.B., Koch, M., Murphy, K.R., Velazquez, Y., Ja, W.W., and Tomchik, S.M. (2016). Neurofibromin Loss of Function Drives Excessive Grooming in Drosophila. G3 (Bethesda) 6, 1083-1093.

bioRxiv preprint doi: https://doi.org/10.1101/834788; this version posted November 8, 2019. The copyright holder for this preprint (which was not certified by peer review) is the author/funder. All rights reserved. No reuse allowed without permission.

499 Klose, A., Ahmadian, M.R., Schuelke, M., Scheffzek, K., Hoffmeyer, S., Gewies, A., Schmitz, F., Kaufmann,
500 D., Peters, H., Wittinghofer, A., and Nurnberg, P. (1998). Selective disactivation of neurofibromin GAP
501 activity in neurofibromatosis type 1. Hum Mol Genet 7, 1261-1268.
502 Koga, M., Yoshida, Y., and Imafuku, S. (2016). Nutritional, muscular and metabolic characteristics in
503 patients with neurofibromatosis type 1. J Dermatol 43, 799-803.
504 Lighton, J.R.B. (2008). Measuring Metabolic Rates: A Manual for Scientists (Oxford: Oxford University
505 Press).
506 Martins, A.S., Jansen, A.K., Rodrigues, L.O., Matos, C.M., Souza, M.L., de Souza, J.F., Diniz Mde, F.,
507 Barreto, S.M., Diniz, L.M., de Rezende, N.A., and Riccardi, V.M. (2016). Lower fasting blood glucose in
508 neurofibromatosis type 1. Endocr Connect 5, 28-33.
509 Masgras, I., Ciscato, F., Brunati, A.M., Tibaldi, E., Indraccolo, S., Curtarello, M., Chiara, F., Cannino, G.,
510 Papaleo, E., Lambrughi, M*., et al.* (2017). Absence of Neurofibromin Induces an Oncogenic Metabolic
511 Switch via Mitochondrial ERK-Mediated Phosphorylation of the Chaperone TRAP1. Cell Rep 18, 659-672.
512 Murphy, K.R., Park, J.H., Huber, R., and Ja, W.W. (2017). Simultaneous measurement of sleep and
513 feeding in individual Drosophila. Nat Protoc 12, 2355-2366.
514 Palgi, M., Greco, D., Lindstrom, R., Auvinen, P., and Heino, T.I. (2012). Gene expression analysis of
515 Drosophilaa Manf mutants reveals perturbations in membrane traffic and major metabolic changes.
516 BMC Genomics 13, 134.
517 Ratner, N., and Miller, S.J. (2015). A RASopathy gene commonly mutated in cancer: the
518 neurofibromatosis type 1 tumour suppressor. Nat Rev Cancer 15, 290-301.
519 Soucy, E.A., van Oppen, D., Nejedly, N.L., Gao, F., Gutmann, D.H., and Hollander, A.S. (2013). Height
520 assessments in children with neurofibromatosis type 1. J Child Neurol 28, 303-307.
521 Souza, M., Jansen, A., Martins, A., Rodrigues, L., and Rezende, N. (2016). Body composition in adults
522 with neurofibromatosis type 1. Rev Assoc Med Bras (1992) 62, 831-836.
523 Souza, M.L.R., Jansen, A.K., Rodrigues, L.O.C., Vilela, D.L.S., Kakehasi, A.M., Martins, A.S., Souza, J.F., and
524 Rezende, N.A. (2019). Increased resting metabolism in neurofibromatosis type 1. Clin Nutr ESPEN 32, 44-
525 49.
526 Stahl, B.A., Peco, E., Davla, S., Murakami, K., Caicedo Moreno, N.A., van Meyel, D.J., and Keene, A.C.
527 (2018). The Taurine Transporter Eaat2 Functions in Ensheathing Glia to Modulate Sleep and Metabolic
528 Rate. Curr Biol 28, 3700-3708 e3704.
529 Stahl, B.A., Slocumb, M.E., Chaitin, H., Diangelo, J.R., and Keene, A.C. (2017). Sleep-dependent
530 modulation of metabolic rate in Drosophila. Sleep.
531 Sullivan, K., El-Hoss, J., Quinlan, K.G., Deo, N., Garton, F., Seto, J.T., Gdalevitch, M., Turner, N., Cooney,
532 G.J., Kolanczyk, M*., et al.* (2014). NF1 is a critical regulator of muscle development and metabolism. Hum
533 Mol Genet 23, 1250-1259.
534 Tennessen, J.M., Barry, W.E., Cox, J., and Thummel, C.S. (2014). Methods for studying metabolism in
535 Drosophila. Methods 68, 105-115.
536 The, I., Hannigan, G.E., Cowley, G.S., Reginald, S., Zhong, Y., Gusella, J.F., Hariharan, I.K., and Bernards, A.
537 (1997). Rescue of a Drosophila NF1 mutant phenotype by protein kinase A. Science 276, 791-794.
538 Tong, J.J., Schriner, S.E., McCleary, D., Day, B.J., and Wallace, D.C. (2007). Life extension through
539 neurofibromin mitochondrial regulation and antioxidant therapy for neurofibromatosis-1 in Drosophila
540 melanogaster. Nat Genet 39, 476-485.
541 Walker, J.A., Gouzi, J.Y., Long, J.B., Huang, S., Maher, R.C., Xia, H., Khalil, K., Ray, A., Van Vactor, D.,
542 Bernards, R., and Bernards, A. (2013). Genetic and functional studies implicate synaptic overgrowth and
543 ring gland cAMP/PKA signaling defects in the Drosophila melanogaster neurofibromatosis-1 growth
544 deficiency. PLoS Genet 9, e1003958.
545 Walker, J.A., Tchoudakova, A.V., McKenney, P.T., Brill, S., Wu, D., Cowley, G.S., Hariharan, I.K., and
546 Bernards, A. (2006). Reduced growth of Drosophila neurofibromatosis 1 mutants reflects a non-cell-

bioRxiv preprint doi: https://doi.org/10.1101/834788; this version posted November 8, 2019. The copyright holder for this preprint (which was not certified by peer review) is the author/funder. All rights reserved. No reuse allowed without permission.

547 autonomous requirement for GTPase-Activating Protein activity in larval neurons. Genes Dev 20, 3311-
548 3323.
549 Williams, J.A., Su, H.S., Bernards, A., Field, J., and Sehgal, A. (2001). A circadian output in Drosophila
550 mediated by neurofibromatosis-1 and Ras/MAPK. Science 293, 2251-2256.
551 Wolman, M.A., de Groh, E.D., McBride, S.M., Jongens, T.A., Granato, M., and Epstein, J.A. (2014).
552 Modulation of cAMP and ras signaling pathways improves distinct behavioral deficits in a zebrafish
553 model of neurofibromatosis type 1. Cell Rep 8, 1265-1270.
554 Xie, K., Colgan, L.A., Dao, M.T., Muntean, B.S., Sutton, L.P., Orlandi, C., Boye, S.L., Boye, S.E., Shih, C.C.,
555 Li, Y.*, et al.* (2016). NF1 Is a Direct G Protein Effector Essential for Opioid Signaling to Ras in the Striatum.
556 Curr Biol 26, 2992-3003.
557 Yang, C.H., Rumpf, S., Xiang, Y., Gordon, M.D., Song, W., Jan, L.Y., and Jan, Y.N. (2009). Control of the
558 postmating behavioral switch in Drosophila females by internal sensory neurons. Neuron 61, 519-526.
559 Yatsenko, A.S., Marrone, A.K., Kucherenko, M.M., and Shcherbata, H.R. (2014). Measurement of
560 metabolic rate in Drosophila using respirometry. J Vis Exp, e51681.

561